Kapal: Jurnal Ilmu Pengetahuan dan Teknologi Kelautan
(Kapal: Journal of Marine Science and Technology)
journal homepage : http://ejournal.undip.ac.id/index.php/kapal
2301-9069 (e)
1829-8370 (p)

Potential Wind Energy Analysis in Maluku Region with Savonius Turbine using CFD Approach

Jandri Louhenapessy[1)], Antoni Simanjuntak[1)], Richard Benny luhulima[2),*)]

[1)] Department of Mechanical Engineering, Faculty of Engineering, Univerisitas Pattimura, Ambon, Indonesia, 97234
[2)] Department of Naval Architecture, Faculty of Engineering, Univerisitas Pattimura, Ambon, Indonesia, 97234
[*)] Corresponding Author : richardluhulima26@gmail.com

Article Info

Keywords:
Savonius Turbine;
Wind Energy;
Maluku Region;
CFD;
Rigid Body Motion;

Article history:
Received: 29/02/2024
Last revised: 28/05/2024
Accepted: 29/05/2024
Available online:30/ 06/2024
Published: 30/06/2024

DOI:
https://doi.org/10.14710/kapal.v21i2.62391

Abstract

The Maluku region, also known as the Moluccas, is an archipelago in Indonesia with exceptional wind patterns ideal for wind power generation. Its strategic location between the Pacific and Indian Oceans creates strong and consistent winds due to temperature differences, making it an optimal site for wind energy production. Harnessing wind power in Maluku can significantly benefit Indonesia and the global renewable energy sector by providing a reliable and sustainable energy source to reduce greenhouse gas emissions and combat climate change. Furthermore, the development of wind power in Maluku could create new economic opportunities and incentives for the local community, promoting sustainable development and reducing the reliance on fossil fuels. A study was conducted to assess the viability of wind energy in Maluku, utilizing a Sonius turbine and computational fluid dynamics (CFD) methodology. By varying the center distance between the Savonius blade radius and its rotational axis, researchers aimed to optimize the turbine's design for maximum energy extraction. The simulations showed that turbine model design significantly impacts performance, with Model 2 outperforming Model 1 due to smoother airflow and more efficient rotation. The pressure distribution on the semicircular blades also influenced turbine performance, with Model 1 producing higher force but slower rotation speed compared to Model 2. The simulations showed that Turbine Model 1 produced a higher average force and power output compared to Turbine Model 2. According to the simulations, Model 1 showcased a higher average power output of 66.5 Watts, while Turbine Model 2 only achieved 46.6 Watts. However, Turbine Model 1 had a slower rotation speed due to its larger radius. Under consistent wind conditions, Turbine Model 1 was capable of producing 5.5% more energy than Turbine Model 2. Choosing an efficient turbine model is crucial for maximising the energy production from wind resources. The findings from this study contribute to a comprehensive understanding of the turbine's behavior and can aid in optimizing its design for maximum energy extraction.

1. Introduction

The Maluku region, also referred to as the Moluccas, is a captivating archipelago situated in Indonesia. This region is renowned for its remarkable and unwavering winds, which make it an ideal location for harnessing wind power, as seen in the East Vietnam Sea [1]. As the world's focus on renewable energy sources, especially wind energy, continues to grow, the potential for utilising abundant wind resources in the Maluku region has become a subject of immense interest. The unique geographical features of the Maluku region contribute to its unique wind patterns. The archipelago is strategically positioned between the Pacific and Indian Oceans, creating a corridor for strong and consistent winds to sweep through the islands. These winds are a result of temperature differences between the two oceans, which generate powerful air currents. The location of the Maluku region within this wind corridor makes it an optimal site for wind-power generation [2].

The potential for harnessing wind power in the Maluku region is significant not only for Indonesia but also for the global renewable energy sector. The consistent winds of the archipelago offer a reliable and sustainable source of energy that can contribute to reducing greenhouse gas emissions and mitigating climate change. By tapping into this renewable resource, the Maluku region has the opportunity to become a leading hub for wind energy production, attract investment, and foster economic growth [3]. The Maluku and North Maluku regions possess a significant amount of untapped potential when it comes to renewable energy sources. Specifically, there are staggering 738 gigawatts of potential energy that can be harnessed from solar, water, wind, and biomass sources. In terms of solar energy alone, the technical potential in these regions was estimated to be approximately 721 gigawatts (GW). Additionally, there is the potential of 1.5 GW from water energy and 75 megawatts from biomass sources. With regard to wind energy, its potential is equally impressive. At a height of 50 m, the regions had the capacity to generate 15.5 gigawatts (GW) of wind energy. This capacity increases to 15.9 GW when the height

is increased to 100 m. However, despite their immense potential, these regions have not yet fully exploited renewable energy sources to maximise their capacity (see Figure 1) [4].

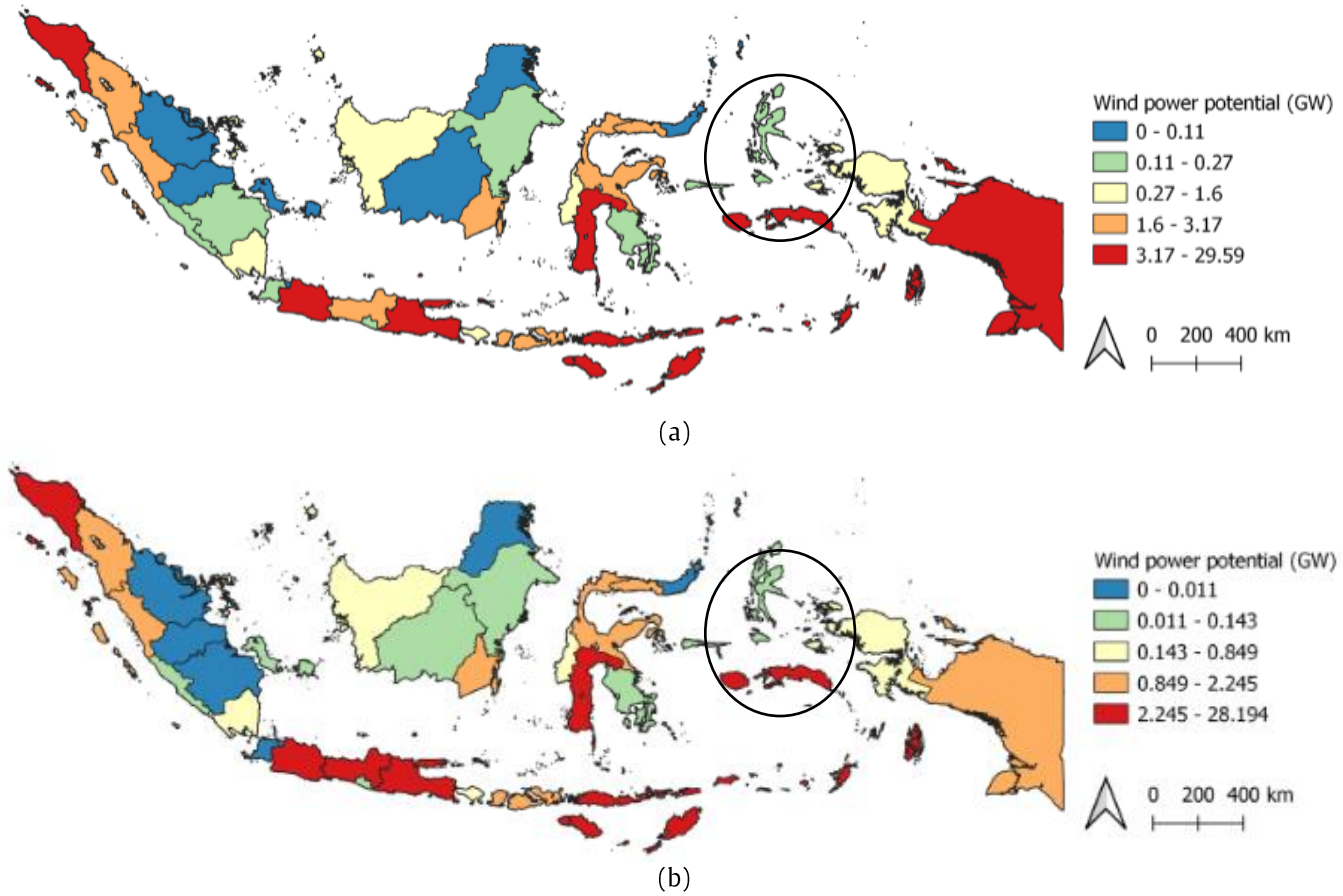

Figure 1. Technical potential of wind power with the minimum mean annual wind speed of (a) 6 m/s at the 50 meters and (b) 6.6 m/s at 100 meters [4]

The potential energy output of Savonius turbines in the Maluku region will be estimated by utilising the collected wind data and computational modelling results. This comprehensive assessment considers the unique design and efficiency characteristics of turbines as well as the specific wind conditions prevalent in the local area. By quantifying the potential energy output, a thorough evaluation of the economic and environmental advantages associated with wind-power generation in a region can be achieved [5]. To begin the estimation process, wind data collected from various sources were analysed and incorporated into the computational model. This will enable us to simulate the behaviour of Savonius turbines under different wind conditions in the Maluku region. By considering factors such as the wind speed, direction, and frequency, we can accurately predict the energy output generated by these turbines [6].

Furthermore, the specific design and efficiency characteristics of Savonius turbines were considered during the estimation process. These turbines are known for their unique vertical-axis design, which allows them to capture wind energy from any direction [7]. In addition, their efficiency in converting wind energy into electrical power is considered, as it directly impacts the overall energy output. The Savonius wind turbine is a type of vertical-axis wind turbine characterised by its unique S-shaped blades. These turbines are designed to capture wind energy from any direction, making them ideal for urban and suburban environments where wind patterns are unpredictable[8]. One of the advantages of the Savonius turbine is its simplicity and ruggedness, which makes it suitable for a wide range of applications including off-grid power generation, water pumping, and ventilation systems. In addition, the low starting torque of the Savonius turbine allows it to efficiently harness wind energy at low wind speeds, making it a practical choice for areas with moderate wind conditions. The design of the Savonius turbine also allows for easy maintenance and installation, making it an accessible option for individuals and small businesses seeking to incorporate wind power into their energy mix. Owing to their reliable performance and versatility, Savonius wind turbines continue to be viable options for sustainable energy generation [9].

This study aims to evaluate the impact of the centre distance of the Savonius blade radius on its rotational axis on the turbine's power output and overall performance. The purpose of this study was to investigate the feasibility of harnessing wind energy in the Maluku region, where the average wind speed is 5 m/s. To accomplish this, archers have used a Sonius turbine as the primary technology for wind-energy conversion. The analysis was based on a computational fluid dynamics (CFD) methodology, which allowed for the examination of different configurations by varying the centre distance between the Savonius blade radius and its rotational axis using two models. The procedures used in this study were based on protocols established in previous studies for conducting CFD simulations [10], [11]. The numerical solution of the fluid flow equations was used to visualise and analyse the complex fluid behaviour around the turbine. Modifying this distance has enabled

turbine models to observe and quantify alterations in flow patterns, pressure distribution, and torque generation, which aids in optimising the turbine design for maximum energy extraction.

2. Methods

2.1. Governing Equation

Computational fluid dynamics, commonly referred to as CFD, was employed to make predictions regarding the force of turbines. Research conducted on forecasting the force of turbine models using computational fluid dynamics (CFD) has yielded remarkable results compared with the outcomes of testing[12]. The CFD model relies on a three-dimensional equation derived from the Reynolds-averaged Navier (RANS) equation to accurately predict the behaviour of fluid flow. Computational fluid dynamics (CFD) has proven to be highly effective in addressing the flow-related challenges encountered in turbine models [13]. By employing a stable incompressible flow, such as that provided by ANSYS-CFX, researchers were able to obtain reliable and precise results. The CFD model allows for a comprehensive analysis of the flow dynamics within the turbine, leading to valuable insights into the forces at play. Overall, the application of computational fluid dynamics (CFD) in predicting the force of turbine models demonstrated its capability to provide accurate and insightful results. The three-dimensional equation derived from the Reynolds-averaged Navier-Stokes (RANS) equation, along with the stable incompressible flow from ANSYS-CFX, contributed to the success of this research. The impressive results obtained through CFD demonstrate its significance in enhancing the understanding of fluid dynamics and its applications in various fields[14].

It was discovered that the selection of turbulence models is critical in the modelling of wake fields. This study used a turbulence model known as the Shear Stress Transport (SST) [15]. Numerous researchers have tested and validated the k–ω SST model and concluded that it produces accurate results [16][17][18]. The RANS solver included in ANSYS CFX was used to solve the fluid flow field. Equations (1), (2), and (3) illustrate the continuity, RANS, and k-ω SST turbulence equations, respectively.

Continuity equation:

$$\frac{\partial \rho}{\partial t} + \frac{\partial}{\partial x_j}(\rho U_j) = 0 \tag{1}$$

where ρ is the fluid density, *t* is time, *and* U_j is the flow velocity vector field.

RANS equation:

$$\rho \bar{f}_i + \frac{\partial}{\partial x_j}\left[-\bar{p}\delta_{ij} + \mu\left(\frac{\partial \bar{u}_i}{\partial x_j} + \frac{\partial \bar{u}_j}{\partial x_i}\right) - \overline{\rho u_i' u_j'}\right] - \rho \bar{u}_j \frac{\partial \bar{u}_i}{\partial x_j} = 0 \tag{2}$$

The mean momentum of a fluid element due to the mean flow unsteadiness is shown on the left side of the RANS equation. That modification is compensated the mean body force ($\bar{f}$), the mean pressure field ($\bar{p}$), the viscous stress, $\mu\left(\frac{\partial \bar{u}_i}{\partial x_j} + \frac{\partial \bar{u}_j}{\partial x_i}\right)$, and apparent stress ($\rho u_i' u_j'$) to the fluctuating velocity field.

Menter′ s SST equation

$$\frac{\gamma}{v_t} P - \beta \rho \omega^2 + \frac{\partial}{\partial x_j}\left[(\mu + \sigma_\omega \mu_t)\frac{\partial \omega}{\partial x_j}\right] + 2(1 - F_1)2\rho_{\omega 2}\frac{1}{\omega}\frac{\partial k}{\partial x_j}\frac{\partial \omega}{\partial x_j} - \left(\frac{\partial(\rho\omega)}{\partial t} + \frac{\partial(\rho u_j \omega)}{\partial x_j}\right) = 0 \tag{3}$$

Menter's SST model is a unique combinationk of–ε and k–ω turbulence models, offering a highly effective formulation that can be applied to a wide range of applications. The aim of this model is to create a robust and efficient model that can accurately capture the complexities of the fluid flow. To achieve this, a blending function, F1, was introduced. This function assigns a value of one to the region close to the solid surface, indicating the dominance of the k–ε model, while assigning a value of zero to the flow domain further away from the wall, indicating the dominance of the k–ω model. In essence, this blending function triggers the k–ε model for the residual flow k and–ω model for the wall region. By incorporating the strengths of both models, the SST model enhanced the free-stream sensitivity and improved the near-wall performance of the k–ω model.

Furthermore, the wind velocity is input according to the prevailing environmental factors in the Maluku Islands, specifically at a rate of 5 m/s. Subsequently, the rotational speed of the axis was determined through computational fluid dynamics (CFD) simulations that employed Rigid Body Motion methodology. This approach allows for a comprehensive analysis of fluid flow dynamics and the resulting impact on the rotational movement of the axis. The power available in the wind stream is influenced by several factors, including air density, area of the wind rotor, and wind velocity. Among these factors, wind velocity has a more significant impact owing to its cubic relationship with the power. The performance of the wind turbine is evaluated using equation

$$P = T * \omega \tag{4}$$

$$T = F * r \tag{5}$$

$$\omega = \frac{2\pi n}{60} \tag{6}$$

This equation represents the relationship between various mechanical parameters, where T represents the mechanical torque in Newton-meters (Nm), ω is the angular speed in radians per second (rad/s), P represents the mechanical power in Watts (W), n represents the shaft rotational speed in revolutions per minute (rpm), r represents the pulley radius in meters

(m), and F represents the force acting on the rotor shaft in Newtons (N). This equation provides a way to calculate the mechanical torque, angular speed, mechanical power, shaft rotational speed, pulley radius, and force acting on the rotor shaft. By using this equation, one can solve for any of these parameters, given the values of the others. Note that the units of each parameter must be consistent for the equation to be valid. This equation is commonly used in mechanical engineering, and plays a crucial role in the analysis and design of various mechanical systems.

2.2. Savonius Turbine Model

The Savonius turbine is considered to be one of the most straightforward wind turbines available. It functions according to the principles of aerodynamics, specifically as a drag-type device [19]. Typically, this turbine is designed with two or three vertical scoops, which are also referred to as blades or buckets, respectively. In contrast to traditional turbines that depend on lift forces, the Savonius turbine operates by harnessing the power of drag forces. When the wind passes through the scoops, it generates torque that causes the central shaft to rotate. This rotation ultimately converts the kinetic energy of the wind into mechanical energy, which can then be used for various applications such as generating electricity or pumping water. The simplicity of the Savonius turbine design makes it an attractive option for locations where more complex wind turbines may not be feasible or cost effective. In addition, its vertical arrangement allows it to capture wind from any direction, making it versatile in terms of wind direction [20].

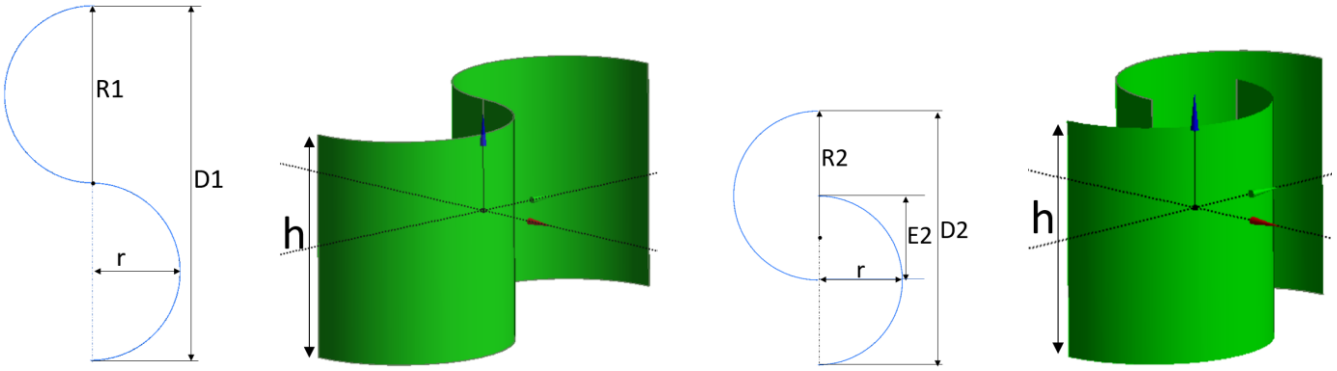

(a) Model 1 (b) Model 2

Figure 2. Turbine Model

Tabel 1 Turbine Particular Properties

Symbol	Parameter	Turbine	Unit
R1	Radius of Turbine Model 1	1.0	m
D1	Diameter of Turbine Model 1	2.0	m
r	Radius of Blade Turbine	0.5	m
h	Height of Blade Turbine	1.0	m
R2	Radius of Turbine Model 2	0.75	m
D2	Diameter ofTurbine Model 2	1.5	m
E2	Inner Distance Between Blades	0.5	m
m	Mass of Turbine	1.33	kg
ρ_{CF}	Density of Carbon Fiber	1700	kg/m^3

The subsequent step involved conducting a simulation using a wind condition map specifically designed for the Maluku Islands. This simulation focused on the wind conditions at a height of 50 m, with a constant speed of 5 m/s. The wind conditions depicted in Figure 3 served as the basis for this simulation, providing a visual representation of the wind patterns in the region. Through this simulation, researchers can gain a deeper understanding of the wind dynamics in the Maluku Islands, which can have significant implications for various applications, such as renewable energy generation, weather forecasting, and climate studies. By accurately modelling the wind conditions at a specific height and speed, valuable information can be obtained to inform decision-making processes and enhance our knowledge of atmospheric processes in this particular region. This simulation serves as a valuable tool for researchers and stakeholders to better understand and utilise the wind resources available on the Maluku Islands.

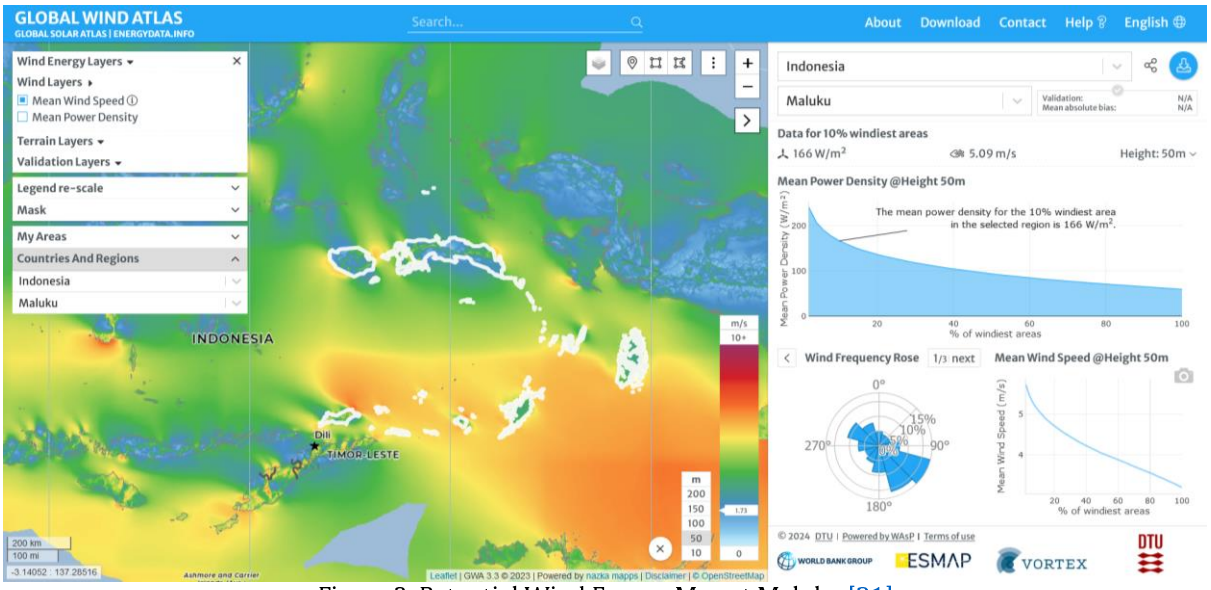

Figure 3. Potential Wind Energy Map at Maluku [21]

2.3. Numerical Domain

The computational domain proposed for this study is a 2D region that extends forward, perpendicular to the front, at the velocity inlet, and 5D towards the rear, perpendicular to the outlet pressure. To mitigate the adverse effects of reverse flow on the boundaries of the domain, we adjusted the transverse and vertical directions to 2D, as suggested in [12]. This adjustment helped to prevent any negative impacts caused by the reverse flow. The domain size and boundary conditions are shown in Figure 4.

In this study, the inlet flow velocity was defined as v= 5 m/s, and the outlet was defined as an outflow fluid. The model is considered rigid and subject to a no-slip condition, which is influenced by wind flow. On the other hand, the bottom, top, and side walls are treated as opening conditions, as depicted in Figure 5. These boundary conditions are crucial for accurately simulating fluid flow within the computational domain and obtaining reliable results.

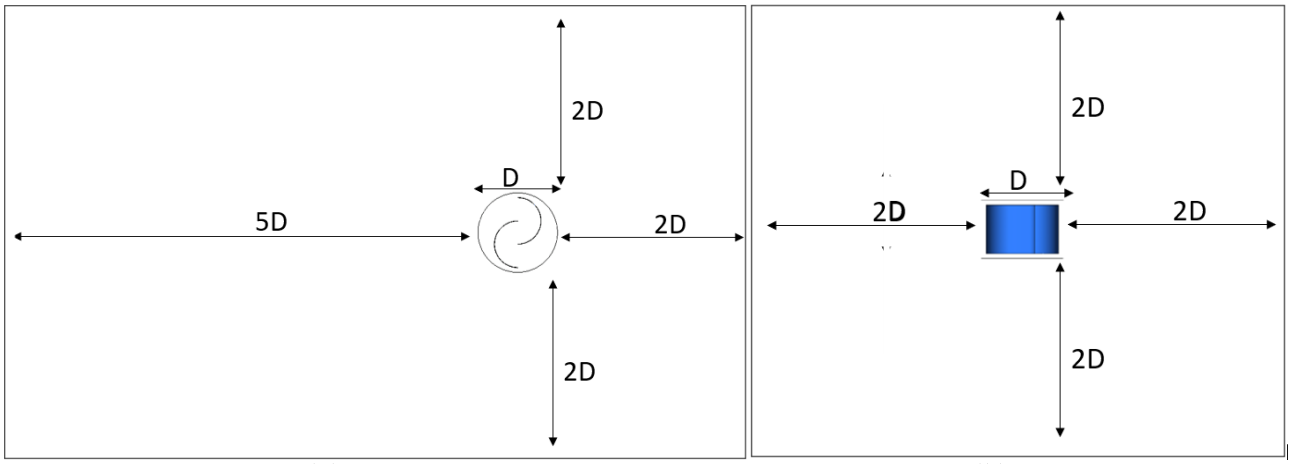

(a) Up view (b) Front view

Figure 4 distance between models and boundary conditions

The proposed computational domain and boundary conditions were carefully designed to ensure accurate and reliable simulations. The adjustments made in the transverse and vertical directions help mitigate the negative impact of reverse flow on the domain boundaries. The specified inlet and outlet conditions, along with the rigid and no-slip conditions for the model, provide a comprehensive framework for studying the fluid dynamics in this system. The opening conditions for the walls further enhance the realism of the simulation.

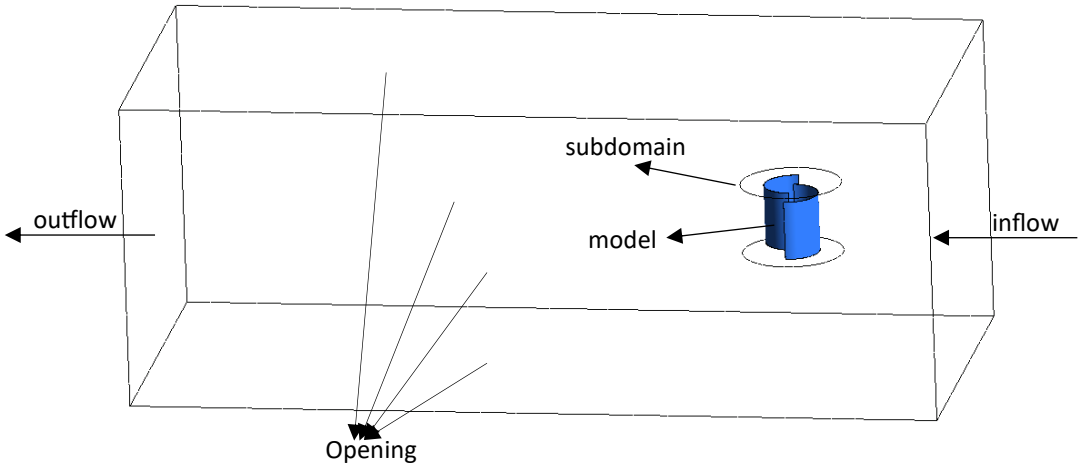

Figure 5. Definition of models and boundary conditions

2.4. Meshing and Grid Convergency

The completion of the mesh construction process for this investigation required the use of a design model. To discretise the computational domain, a combination of structured and unstructured meshes was utilised. A mesh composed of triangular elements was created on the model surface to account for the intricate geometrical features of the model. Subsequently, the boundary layer was refined by incorporating prism elements generated by expanding the surface mesh node. To populate the area near the model, inflated tetrahedral elements were employed, whereas an unstructured mesh with grid generation was utilised to decrease the overall number of components in the distant field.

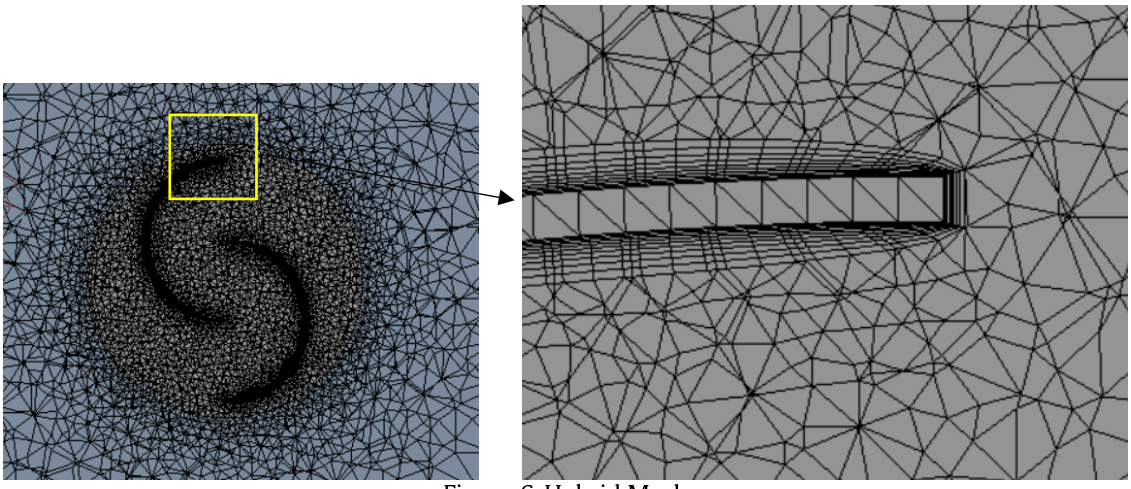

Figure 6. Hybrid Mesh

Although a fine mesh can provide reliable results in ANSYS CFX, it also leads to increased computational costs and time consumption owing to the large number of elements. The size of the mesh played a crucial role in the calculation process. To ensure mesh convergence, this was performed on the submarine model, as depicted in Figure 6 Through this process, an optimal mesh convergence was achieved, resulting in a total mesh count of 1.89 million. This convergence was validated by Anderson's findings, which indicated a difference of less than 2% in the total resistance coefficient.

2.5. Rigid Body Motion

The Computational Fluid Dynamics (CFD) technique was employed to accurately analyse and understand the flow characteristics both around and inside the turbine. This method allows for precise simulation and optimisation of turbine performance. By utilising the accurate results obtained from CFD analysis, an optimisation methodology can be implemented to determine the most suitable solution for the turbine. Simulating the flow around the Savonius rotor poses a significant challenge because of the highly time-dependent conditions involved. Additionally, the flow separation phenomenon significantly influences the power coefficient of the rotor. Therefore, it is crucial to employ a numerical procedure to ensure the accuracy. The first step in this process is to thoroughly validate the model and entire numerical procedure. In this study, the ANSYS-CFX software was utilised to conduct all simulations.

Given the unsteady nature of the flow characteristics around the Savonius turbine, unsteady Reynolds-averaged Navier–Stokes equations were employed. These equations were solved using the Rhie-Chow algorithm for pressure-velocity coupling. To solve for the various variables and turbulent values, a second-order upwind scheme was utilised in a finite-volume formulation. A realisable SST model, which is commonly recommended for rotating zones, was used to model the turbulence parameters. Moreover, a highly accurate mesh for the 3D Savonius turbine was employed in this study. To solve the unsteady flow characteristics, both the Rigid Body Motion (RBM) and Sliding Mesh Model (SMM) were utilised. The

simulations were conducted with a constant time step to ensure that four complete revolutions were always computed. The effect of the time step on the CFD simulation was also investigated to ensure accurate results.

The Rigid Body Motion (RBM) approach was used to simulate the movement of solid bodies within the fluid domain. This technique allows for an accurate representation of the motion and interaction of rigid objects such as rotating components or moving boundaries. By incorporating the RBM, researchers can capture the dynamic behaviour of the system and analyse its effects on flow characteristics. Additionally, a Sliding Mesh Model (SMM) was employed to simulate the relative motion between different regions of the computational domain. This technique enables researchers to accurately model scenarios with sliding or rotating interfaces. By utilising the SMM, researchers can effectively capture the complex interactions between different fluid regions and accurately predict the flow behaviour.

3. Results and Discussion

The computational fluid dynamics approach was employed to conduct the simulation, which involved the use of the rigid-body motion method. This method leads to the generation of distinct rotations, as shown in Figure 7. Model 1 exhibited an angular speed of 21 revolutions per minute, whereas Model 2 demonstrated a higher angular speed of 28 revolutions per minute. The dissimilarity in the rotation outcomes can be attributed to the variance in turbine radius lengths. Specifically, Model 1 had a turbine length that was 25% greater than that of Model 2.

The computational fluid dynamics approach allows for a detailed analysis of the fluid flow around the turbines, considering factors such as velocity, pressure, and turbulence. By utilising numerical methods, the simulation could accurately predict the behaviour of the fluid and the resulting rotations of the turbines. The rigid body motion method was particularly useful in this simulation, as it enabled the turbines to undergo distinct rotations. This method allowed for the examination of how the turbines interacted with the fluid flow and how their rotations were influenced by factors such as the turbine length.

Overall, the simulation results highlight the importance of considering the turbine design and dimensions when analysing their performance. The differences in angular speeds between Models 1 and 2 underscored the impact of the turbine radius length on the rotation outcomes. By employing computational fluid dynamics and the rigid body motion method, this study provides valuable insights into the behaviour of turbines in fluid flow environments.

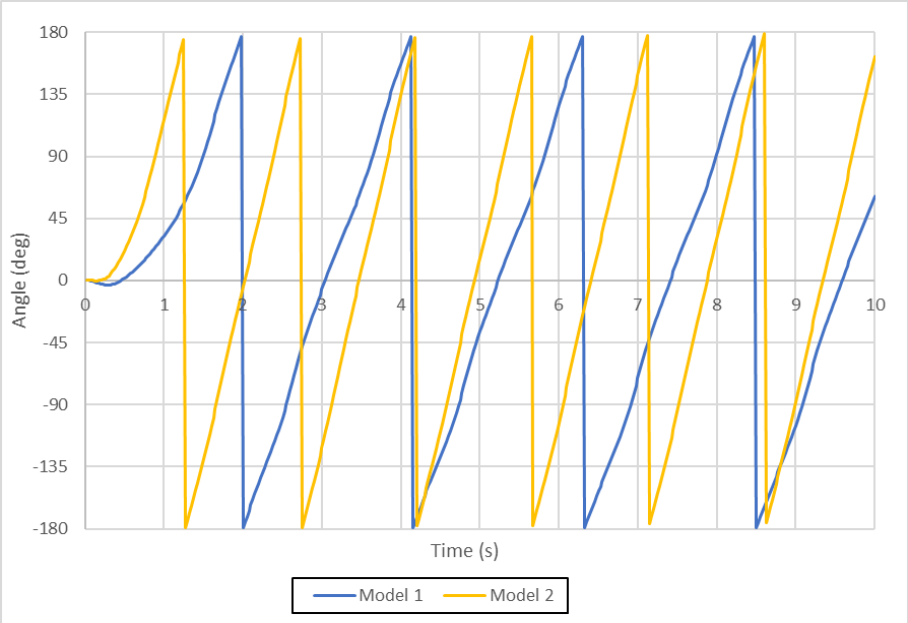

Figure 7. turbine rotation

The disparity in the length and placement of the turbine has a significant impact on the performance of the two models. The Model 1 turbine, as depicted in Figure 8 (a), encounters difficulties during its initial start owing to inadequate airflow. This is primarily attributed to the turbine length and position, which hinder the proper flow of air. Consequently, the Model 1 turbine operates at a slower speed than its counterpart. In contrast, the Model 2 turbine (Figure 8 (b)) exhibits a more favourable performance. The air flow in this turbine appears to be well distributed and efficient, particularly during the initial rotation. This can be attributed to the optimal length and position of the turbine, which facilitates smooth and effective rotation. As a result, the Model 2 turbine operates at a higher speed and demonstrates improved performance compared to the Model 1 turbine.

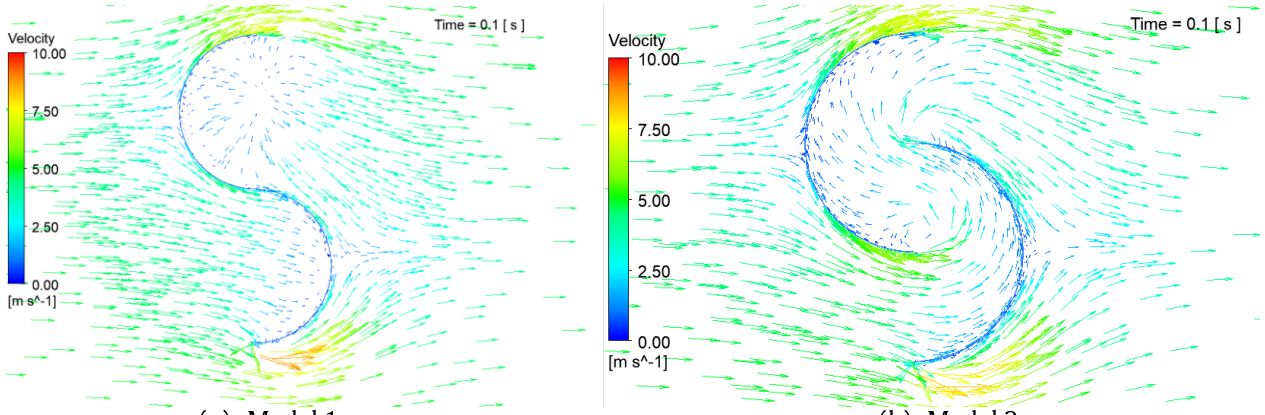

(a) Model 1 (b) Model 2

Figure 8. Flow Velocity

The difference in the performance of the two turbines can be attributed to variations in their designs and configurations. The length and position of the turbine play a crucial role in determining the efficiency of the airflow and subsequent rotation. In the case of the Model 1 turbine, the improper flow of air during the initial start hampers its performance, resulting in a slower rotation. On the other hand, the Model 2 turbine benefits from a well-designed length and position, allowing for a smooth and efficient airflow, leading to a more effective rotation and higher speed. Therefore, it is evident that the difference in the length and position of the turbines significantly influences their respective performance.

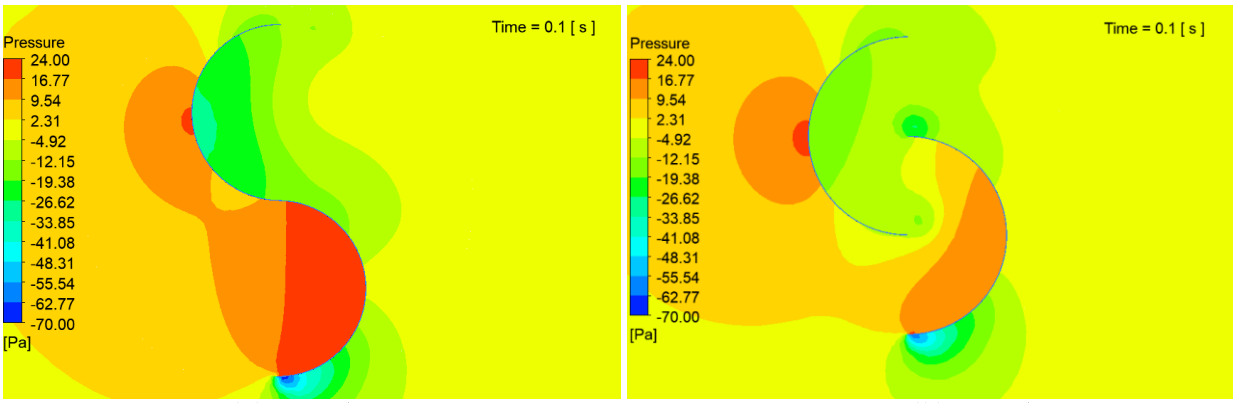

(a) Model 1 (b) Model 2

Figure 9. Pressure Distribution

The arrangement of the semicircular blades on the Savonius turbine had a significant impact on the pressure distribution in the two different models. Figure 9 (a) shows that the air pressure is concentrated predominantly in the direction of the turbine inlet. This concentration of pressure contributes to the turbine's ability to rotate because it adds a substantial amount of weight to the turbine. This increased weight enabled the turbine to rotate efficiently and generate power. However, in turbine model 2 (Figure 8 (b)), the pressure distributions were different. The pressure was distributed across the first curve of the turbine and then flowed to the other curves. This pressure distribution allows for an easier rotation of the turbine. The pressure is evenly distributed throughout the turbine, facilitating smoother rotation and enhancing the overall performance of the turbine.

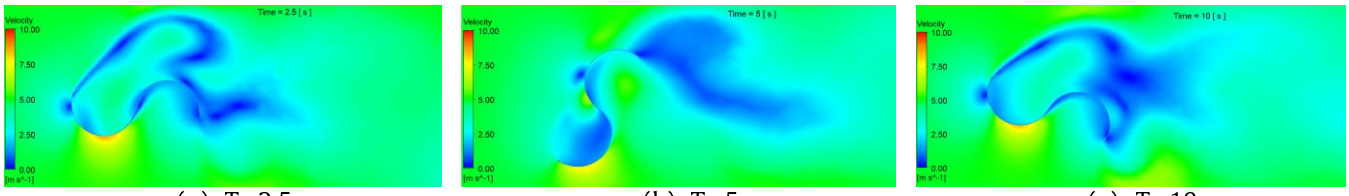

(a) T= 2.5 s (b) T= 5 s (c) T= 10 s

Figure 10. rotating motion Turbin Model 1

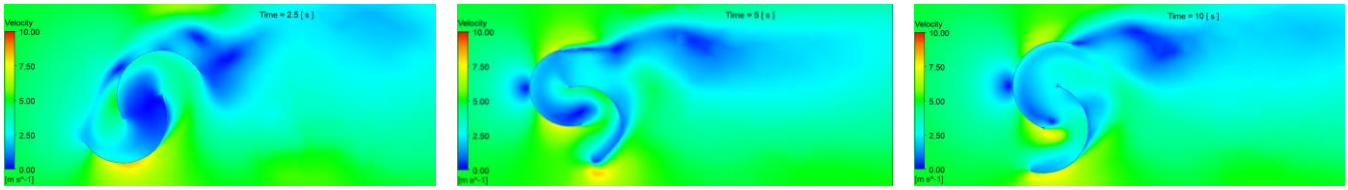

T= 2.5 s T= 5 s T= 10 s

Figure 11. rotating motionTurbine Model 2

To further illustrate the rotation processes of the two turbine models, Figure 10 shows the rotation process of Turbine Model 1, while Figure 11 shows the rotation process of Model 2. These figures provide visual representations of how the turbines rotate under the influence of the pressure concentrations and distributions, as discussed earlier. By studying these rotation processes, researchers and engineers can gain valuable insights into the performance characteristics of each turbine model and make informed decisions regarding their design and optimisation. Thus, the positioning of the semicircular blades on the Savonius turbine plays a crucial role in determining the pressure concentration and distribution within the turbine. These factors directly affect the ability of the turbine to rotate efficiently. By analysing the pressure patterns and studying the rotation processes of different turbine models, researchers can enhance their understanding of turbine performance and make improvements to optimise their design.

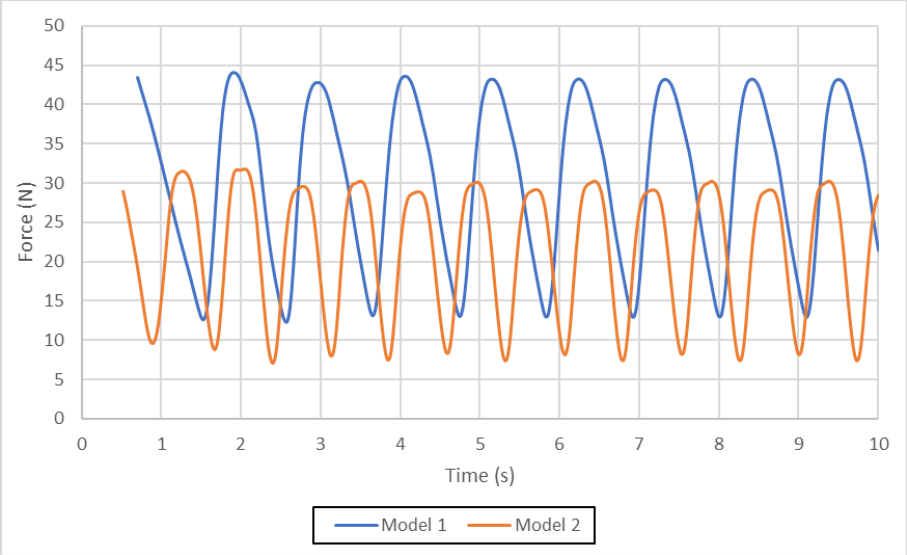

Figure 12. Force Calculation

The power generated by the rotation of a turbine owing to wind is a result of the force exerted by the wind on the turbine blades. Figure 12 illustrates that turbine model 1 produces an average force of 30.7 N, while turbine model 2 produces an average force of 21.3 N. This discrepancy in force production between the two models is substantial, with turbine model 1 generating a force that is 31% higher than that of turbine model 2. Despite the significant difference in force production between the two turbine models, it is interesting to note that the rotation speed of turbine model 1 was 31% slower than that of turbine model 2. This variation in the rotation speed can be attributed to the fact that the radius of the turbine arm in Model 1 is 25% larger than that of Model 2. This difference in arm length directly impacts the rotational speed of the turbine blades, resulting in the observed decrease in the rotation speed for Model 1 compared to Model 2. The relationship between the force production and rotation speed in the two turbine models highlights the intricate balance between the design factors in wind turbine technology. Although turbine model 1 generates a higher force output, this comes at the cost of a slower rotation speed owing to the larger radius of its turbine arm. Understanding these trade-offs is crucial for optimising wind turbine performance and efficiency, as designers must carefully consider the impact of design choices on both force production and rotation speed to achieve the desired balance in turbine operation.

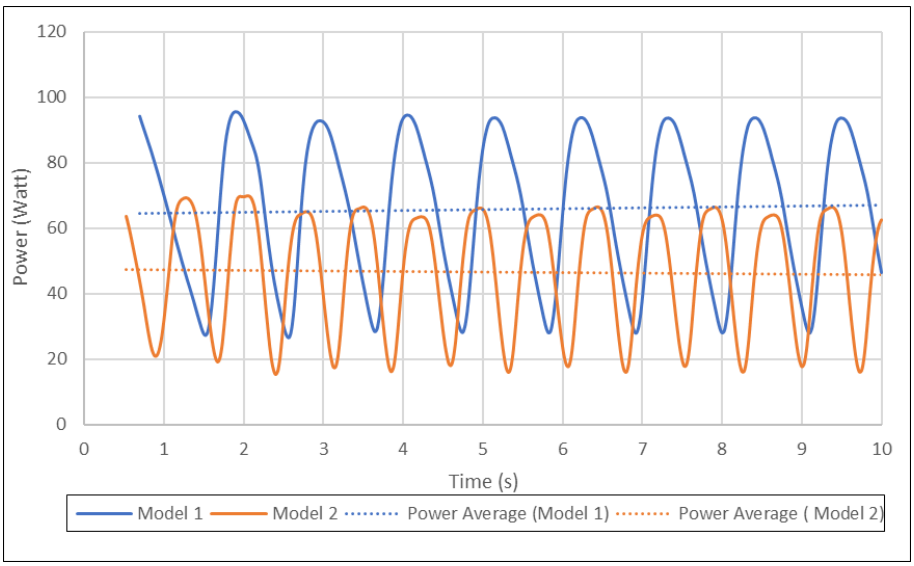

Figure 13. Power Calculation

The simulations conducted on the two distinct turbine models revealed significant differences in their average power outputs, as shown in Figure 13. Turbine model 1 was found to have an average power output of 66.5 Watts, whereas turbine model 2 exhibited a lower average power output of 46.6 Watts. These results indicate that turbine model 1 is more efficient in converting wind energy into electrical power than turbine model 2 is. In a scenario where the wind speed remained constant at 5 m/s for 1 h, the energy production capabilities of the two turbine models were further evaluated. Turbine model 1 was able to generate 83 kilowatt-hours (kWh) of energy under these conditions, while turbine model 2 produced a slightly lower amount of 78 kWh. This demonstrates that turbine model 1 had a higher energy production capacity when subjected to consistent wind conditions. A comparison of the energy production between the two turbine models revealed that turbine model 1 was capable of producing 5.5% more energy than turbine model 2 under the specified conditions. These findings underscore the importance of selecting an efficient turbine model to maximise energy production from wind resources. The simulations conducted provide valuable insights into the performance differences between turbine models and highlight the significance of choosing the most suitable technology for effectively harnessing wind energy.

4. Conclusion

The computational fluid dynamics approach, using the rigid body motion method, was employed to simulate the two turbine models. Model 1 had a turbine radius 25% larger than Model 2, resulting in an angular speed of 21 revolutions per minute for Turbine Model 1 and 28 revolutions per minute for Model 2. The simulation accurately predicted the behaviour of the fluid and the resulting turbine rotations. Turbine Model 1 experienced difficulties during the initial start owing to the inadequate airflow caused by its length and position. Conversely, Turbine Model 2 had a smoother and more efficient airflow, leading to an improved performance and higher speed. The length and position of the turbines significantly influence their performance.

The arrangement of the semicircular blades on the Savonius turbine affects the pressure distribution. In Turbine Model 1, the air pressure was concentrated predominantly in the direction of the turbine inlet, contributing to its ability to rotate. Turbine Model 2 had pressure distributed across the first curve of the turbine, allowing for easier rotation. Turbine Model 1 produced a higher average force of 30.7 N compared to Turbine Model 2's 21.3 N, but Turbine Model 1's rotation speed was slower due to its larger radius. The relationship between force production and rotation speed highlights the intricate balance between the design factors in wind turbine technology. Simulations revealed that Model 1 had a higher average power output of 66.5 Watts compared to Turbine Model 2's 46.6 Watts, and Turbine Model 1 was capable of producing 5.5% more energy than Turbine Model 2 under consistent wind conditions. The simulation results highlight the significance of considering various factors, such as blade design and aerodynamics, when designing wind turbines for optimal energy production. Therefore, it is crucial to carefully consider the dimensions and placement of turbines to optimise their efficiency and output. In conclusion, the design and layout of wind turbines play a critical role in achieving maximum energy production, and should be approached with a comprehensive understanding of the various factors that influence their performance.

Acknowledgment

The authors would like to express their gratitude to the team at the numerical modelling laboratory of the Faculty of Engineering at Pattimura University for their valuable support throughout the study. The authors acknowledge the significant contribution of the laboratory team to ensuring the success of this research project.

References

[1] N. X. Tung, D. H. Cuong, B. T. B. Anh, N. T. Nhan, and T. Q. Son, "Combining QuickSCAT wind data and Landsat ETM+ images to evaluate the offshore wind power resource of East Vietnam Sea," *Vietnam Journal of Marine Science and Technology*, vol. 20, no. 2, pp. 143–153, 2020, doi: 10.15625/1859-3097/20/2/14714.

[2] D. Pelupessy and F. Manuhutu, "Hybrid solar-wind-diesel power plant for small islands in Maluku Province," *IOP Conf Ser Earth Environ Sci*, vol. 339, no. 1, p. 012046, 2019, doi: 10.1088/1755-1315/339/1/012046.

[3] L. C. S. Rocha, P. R. Junior, and A. Maheri, "Economic analysis of the wind energy generation," in *Renewable Energy Production and Distribution Volume 2*, Elsevier, 2023, pp. 183–214. doi: 10.1016/B978-0-443-18439-0.00006-9.

[4] H. D. Puspitarini, "Beyond 443 GW: Indonesia' s infinite renewables energy potentials," Jakarta, 2021.

[5] M. A. Kamoji, S. B. Kedare, and S. V. Prabhu, "Performance tests on helical Savonius rotors," *Renewable Energy*, vol. 34, no. 3, pp. 521–529, 2009, doi: 10.1016/j.renene.2008.06.002.

[6] M. B. Salleh, N. M. Kamaruddin, Z. Mohamed-Kassim, and E. A. Bakar, "Experimental investigation on the characterization of self-starting capability of a 3-bladed Savonius hydrokinetic turbine using deflector plates," *Ocean Engineering*, vol. 228, 2021, doi: 10.1016/j.oceaneng.2021.108950.

[7] M. H. Mohamed, G. Janiga, E. Pap, and D. Thèvenin, "Optimization of Savonius turbines using an obstacle shielding the returning blade," *Renewable Energy*, vol. 35, no. 11, pp. 2618–2626, 2010, doi: 10.1016/j.renene.2010.04.007.

[8] M. Tartuferi, V. D' Alessandro, S. Montelpare, and R. Ricci, "Enhancement of savonius wind rotor aerodynamic performance: A computational study of new blade shapes and curtain systems," *Energy*, vol. 79, no. C, pp. 371–384, 2015, doi: 10.1016/j.energy.2014.11.023.

[9] J.-L. Menet, "Aerodynamic Behaviour of a New Type of Slow-Running VAWT," *Wind Energy*, pp. 235–240, 2007, doi: 10.1007/978-3-540-33866-6_43.

[10] A. Rizzi and J. Vos, "Toward Establishing Credibility in Computational Fluid Dynamics Simulations," *AIAA Journal*, vol. 36, no. 5, pp. 668–675, 1998, doi: 10.2514/2.442.

[11] K. Mullenix, D. K. Walters, A. Villegas, and F. J. Diez, "Investigation of Turbulence Model Performance in Computational Fluid Dynamics Simulations of Horizontal Axis Wind Turbines," in *Volume 3: Computational Fluid Dynamics; Micro and Nano Fluid Dynamics*, American Society of Mechanical Engineers, 2020. doi: 10.1115/FEDSM2020-20269.

[12] A. Ramadan, M. Hemida, W. A. Abdel-Fadeel, W. A. Aissa, and M. H. Mohamed, "Comprehensive experimental and numerical assessment of a drag turbine for river hydrokinetic energy conversion," *Ocean Engineering*, vol. 227, 2021, doi: 10.1016/j.oceaneng.2021.108587.

[13] B. Belkacem and M. Paraschivoiu, "CFD Analysis of a Finite Linear Array of Savonius Wind Turbines," *Journal of Physics: Conference Series*, vol. 753, no. 10, 2016, doi: 10.1088/1742-6596/753/10/102008.

[14] W. Shi, M. Atlar, R. Norman, B. Aktas, and S. Turkmen, "Numerical optimization and experimental validation for a tidal turbine blade with leading-edge tubercles," *Renewable Energy*, vol. 96, pp. 42–55, 2016, doi: 10.1016/J.RENENE.2016.04.064.

[15] F. R. Menter, "Two-equation eddy-viscosity turbulence models for engineering applications," *AIAA Journal*, vol. 32, no. 8, pp. 1598–1605, 1994, doi: 10.2514/3.12149.

[16] F. R. Menter, M. Kuntz, and R. Langtry, "Ten Years of Industrial Experience with the SST Turbulence Model," in *4th Internal Symposium, Turbulence, heat and mass transfer*, New York, Wallingford: Begell House, 2003, pp. 625–632.

[17] I. K. A. P. Utama, W. D. Aryawan, A. Nasirudin, Sutiyo, and Yanuar, "Numerical Investigation into the Pressure and Flow Velocity Distributions of a Slender-Body Catamaran Due to Viscous Interference Effects," *International Journal of Technology*, vol. 12, no. 1, p. 149, 2021, doi: 10.14716/ijtech.v12i1.4269.

[18] F. zhi Zeng, J. ping Li, Y. Wang, M. Sun, and C. Yan, "Parametric uncertainty quantification of SST turbulence model for a shock train and pseudo-shock phenomenon," *Acta Astronautica*, vol. 196, pp. 290–302, 2022, doi: 10.1016/J.ACTAASTRO.2022.05.002.

[19] V. Dhamotharan, R. Meena, P. Jadhav, P. Ramu, and K. A. Prakash, "Robust Design of Savonius Wind Turbine," in *Renewable Energy in the Service of Mankind Vol I*, Cham: Springer International Publishing, 2015, pp. 913–923. doi: 10.1007/978-3-319-17777-9_82.

[20] N. K. Sarma, A. Biswas, and R. D. Misra, "Comparative Assessment of Savonius Water Turbine With Conventional Savonius Wind Turbine," in *Volume 1: Compressors, Fans, and Pumps; Turbines; Heat Transfer; Structures and Dynamics*, American Society of Mechanical Engineers, 2019. doi: 10.1115/GTINDIA2019-2459.

[21] globalwindatlas.info, "Global Wind Atlas: MAluku Area, Indonesia," Global Wind Atlas. Accessed: Feb. 10, 2024. [Online]. Available: https://globalwindatlas.info/en/area/Indonesia/Maluku